Naval Research Laboratory
Washington, DC 20375-5320

NRL/FR/6110--00-9945

Obscurants for Infrared Countermeasures II

J.C. Owrutsky
H.H. Nelson
H.D. Ladouceur
A.P. Baronavski

Chemical Dynamics and Diagnostics Branch
Chemistry Division

March 24, 2000

REPORT DOCUMENTATION PAGE

Form Approved
OMB No. 0704-0188

1. AGENCY USE ONLY (*Leave Blank*)	2. REPORT DATE	3. REPORT TYPE AND DATES COVERED
	March 24, 2000	Interim Report (1998-1999)

4. TITLE AND SUBTITLE

Obscurants for Infrared Countermeasures II

5. FUNDING NUMBERS

61153N
BE033-02-4K

6. AUTHOR(S)

J.C. Owrutsky, H.H. Nelson, H.D. Ladouceur, and A.P. Baronavski

7. PERFORMING ORGANIZATION NAME(S) AND ADDRESS(ES)

Naval Research Laboratory
Washington, DC 20375-5320

8. PERFORMING ORGANIZATION REPORT NUMBER

NRL/FR/6110--00-9945

9. SPONSORING/MONITORING AGENCY NAME(S) AND ADDRESS(ES)

Office of Naval Research
800 North Quincy Street
Arlington, VA 22217-5660

10. SPONSORING/MONITORING AGENCY REPORT NUMBER

11. SUPPLEMENTARY NOTES

12a. DISTRIBUTION/AVAILABILITY STATEMENT

Approved for public release; distribution is unlimited.

12b. DISTRIBUTION CODE

13. ABSTRACT (*Maximum 200 words*)

This report describes results of a search for a suitable mid-infrared obscurant. The goal is to identify a material with sufficient extinction, equivalent or superior to brass, which has been demonstrated to provide high extinction but without its toxicity and environmental effects. More than ten materials were initially selected as promising based on results from previous studies or from the bulk spectra or optical constants. These powders were characterized by laboratory extinction using the previously constructed NRL apparatus in which infrared transmission and mass loading are determined for dry powder samples in a flowing gas stream. The average particle sizes were characterized, and the extinction coefficients are compared to calculated values. Of the materials tested, graphite with a nominal 2-micron average particle diameter has the highest mass-extinction coefficient. Results of field test studies of obscurant materials are also reported.

14. SUBJECT TERMS

Obscurant Infrared countermeasure
Powder extinction

15. NUMBER OF PAGES

31

16. PRICE CODE

17. SECURITY CLASSIFICATION OF REPORT	18. SECURITY CLASSIFICATION OF THIS PAGE	19. SECURITY CLASSIFICATION OF ABSTRACT	20. LIMITATION OF ABSTRACT
UNCLASSIFIED	UNCLASSIFIED	UNCLASSIFIED	UL

NSN 7540-01-280-5500

Standard Form 298 (Rev. 2-89)
Prescribed by ANSI Std 239-18
298-102

CONTENTS

EXECUTIVE SUMMARY E1

INTRODUCTION 1

TECHNICAL APPROACH 2

Overview 2
Background 3
Methods 7

EXPERIMENTAL 8

LABORATORY RESULTS 9

Particle Size Measurements 9
Measured Extinction Coefficients for Obscurant Candidates 11

DISCUSSION 13

FIELD MEASUREMENTS 17

CONCLUSIONS 19

ACKNOWLEDGMENTS 19

REFERENCES 20

APPENDIX A – Distribution-Averaged Mass-Extinction Coefficients 23

APPENDIX B – Calculated Extinction for Gases: A Possible Alternative to Powders 25

APPENDIX C – Calculated Mass-Extinction Coefficients for Silica, Alumina, and Silicon Carbide 27

EXECUTIVE SUMMARY

Effective mid-infrared obscurant materials are needed by the Navy as countermeasures against heat-seeking, antiship missile (ASM) attack. Successful obscuring materials must not only exhibit extinction in the spectral regions of interest, 3-5 and 8-12 μm, but also satisfy other criteria with respect to toxicity, environmental impact, ease of deployment, and availability. The Army and others have demonstrated that brass exhibits favorable obscuration properties. But this material is highly toxic and environmentally detrimental. The goal of this work is to find an infrared obscurant material that provides extinction that is equivalent or superior to brass but without its toxicity and environmental effects.

Previous results from this laboratory demonstrated that the initial candidate obscurant materials boron nitride and boric acid exhibit extinction coefficients that are inferior to those of brass (Ladouceur et al., 1997; Ladouceur et al., 1998). This report describes results of the ongoing search for a suitable infrared (IR) obscurant. Materials were selected and then characterized by laboratory extinction measurements. The latter were performed using the NRL apparatus in which dry powder samples are entrained into a flowing gas stream such that the mass loading can be determined and the powders' extinction measured by Fourier transform infrared (FTIR) spectroscopy. Bulk material spectra and optical constants were used to guide the choice of candidate materials. Average particle size and, when possible, distribution were chosen to optimize the extinction in the infrared regions of interest.

Of the materials tested, graphite with a nominal 2-μm average particle size has the highest mass-extinction coefficients, σ_m (approximately 0.72 m^2/g in both spectral bands). These values are higher than those measured previously at NRL for brass (0.34 m^2/g). Graphite has a lower packing density than brass, however, so that it also has a lower volume-extinction coefficient. The effectiveness of an obscurant may best be represented either by the volume-extinction coefficient or the mass-extinction coefficient, depending on how the material is deployed. Graphite is the superior overall choice of material because of its much lower toxicity and environmental impact.

In addition to laboratory measurements, field studies were conducted. These were primarily intended to test the screen cartridges used to deploy the materials. All of the cartridges fired successfully. The cartridges were loaded with the same volume of nine materials to evaluate how they dispersed and to provide preliminary information on the extinction of the clouds generated. Various materials were tested, including metal (brass), metal oxides, semiconductors, polymers, and an inorganic salt. Absolute extinction measurements were precluded because shortly after the rounds were fired, the clouds were optically thick. Nevertheless, the results indicated that most but not all of the materials performed as suitable obscurant materials under the field test conditions.

OBSCURANTS FOR INFRARED COUNTERMEASURES II

INTRODUCTION

A promising approach to the development of countermeasures against emerging threats such as imaging infrared (IR) seekers is to successfully combine obscuration and decoy technologies with modern deployment capabilities such as unmanned airborne vehicles. Emerging seekers use focal plane arrays (to discriminate for extended sources) that can operate in several infrared bands (3-5 and 8-12 μm) and thus provide a greater challenge with respect to spectral balance and deployment capability than before. Obscuration countermeasures are intended to mask the thermal signature of a target by deploying a material that has low infrared transmission between the seeker and the target. Brass performs well as an obscurant material based solely on infrared attenuation (Edwards et al., 1992), but it also has undesirable toxicological properties (Haley and Kurnas, 1993). The work reported here is motivated by the need for an effective infrared obscuration material with comparable or better extinction capabilities than brass but without the detrimental environmental impact. These obscuration materials will be an integral component of the NRL Vertically Launched Imaging Infrared Decoy Technologies (VLD) Program.

This work continues and extends previous work at NRL on identifying suitable obscurant materials for infrared countermeasures (Ladouceur et al., 1997). The original study focused on brass, which has been investigated and is currently used by the Army (Embury et al., 1994), and two newly investigated materials, boric acid and boron nitride. The extinction coefficients were measured in the laboratory and neither material has a high enough extinction to be useful. Quantitative extinction measurements are challenging because it is difficult to measure the transmission of a gas-suspended dry powder under conditions in which the mass loading can be determined. The previous NRL report provides a description of the experimental apparatus used to measure the extinction coefficients. It also relates the theory and numerical calculations of extinction as a function of particle size distribution and indices of refraction. The NRL apparatus has also been used to investigate the near-IR extinction of titanium oxide (Ladouceur et al., 1999). In this case, several samples with different size distributions were investigated. The results illustrate that the particle size distribution dramatically affects the extinction properties. The experimental methods and apparatus for measuring the extinction coefficients in this work are the same as those described in previous reports.

In the present study, candidate obscurant materials were selected because they either exhibited high extinction in previous studies or they were considered to have promising optical properties based on reported indices of refraction (e.g., Palik (1984)) or IR absorption spectra for the bulk material (e.g., Nyquist and Kagel, 1971). Various classes of materials were considered. Calculations of the extinction coefficients guided the choice of materials and target particle sizes to optimize the extinction. Samples were evaluated by laboratory extinction coefficient measurements. The particle size distribution was characterized for many samples. The measured extinction coefficients and size distribution are compared to extinction calculations as a function of particle size to determine whether modifying the size distribution for that material would increase the extinction enough to constitute a viable obscurant material. The best obscurant material found to date is 2-μm diameter graphite. Iron oxide and monoammonium phosphate (MAP) also exhibit relatively high mass-extinction coefficients (σ_m). For the

Manuscript approved January 7, 2000.

latter two, the particle sizes are not optimal so that samples with a different size distribution may yield a satisfactory obscurant. All the higher extinction materials mentioned are much less toxic than brass.

The nature of the obscurant deployment affects the size distribution of the particles and thereby the extinction. Field tests are important to verify that results in the laboratory are applicable to the practical obscurant implementation. Field tests were conducted to confirm the functioning of screen cartridges used to deploy the material and establish a correspondence between the extinction measured in the laboratory and that realized in the field.

TECHNICAL APPROACH

Overview

There are several criteria for selecting an obscurant material; their relative importance depends on how the material will be deployed. Favorable extinction and optical properties are critical for selecting an infrared obscurant material, but other properties are also important. These include toxicological properties and environmental impact (on the ship, sailors, and marine life), availability, cost, ease of deployment, and resilience to deployment conditions. Some materials, such as those commonly used as abrasives (silicon carbide, aluminum oxide), are attractive because they are cheap and commercially available – not only in large quantities, but also in small (1-10 μm) particle sizes with narrow size distributions. Inorganic salts can have various constituents (ions) that can be used to tune the optical properties. These latter materials are difficult to obtain as small particles with narrow size distributions. Oxides and semiconductors lack hydrogens so they typically do not have strong (vibrational) absorption bands in the 3-5 μm region. Many salts, on the other hand, have hydrogen-containing ions such as ammonium, and some exhibit strong absorptions in the 3-5 μm region. There are general trends regarding toxicity and environmental impact. Metals are not only a biohazard but also threaten the electrical systems of the ship being obscured. Toxological studies have shown that brass is highly toxic (rated 9 on an Environmental Protection Agency (EPA) scale of 0-9 (Haley and Kurnas, 1993)). Graphite (EPA = 4) is much less so, and titanium oxide and salts are virtually nontoxic (EPA = 0).[1]

The utility of laboratory studies depends on the correlation between extinction coefficients measured in the laboratory and extinction realized in the field. An important factor in this correlation is the similarity in the particle size distribution of the material. The actual particle size distribution can be sensitive to how the powder is dispersed.[2] If particles are dispersed violently in the laboratory, such that they approach the primary particle size, then the measured extinction will usually be near the best case (except in the rare case of sizes much smaller than the optimum). The assumed extinction will then be greater than what is actually realized. In the NRL apparatus, powders are lifted relatively gently and entrained in a gas stream. Here, there may be more clumping so that the extinction coefficients are probably underestimated (and lower than in other reports). Therefore, countermeasure devices based on these measurements should provide the intended extinction, if not more.

How obscurant materials are selected and optimized depends on whether the amount of material (or payload for the method of deployment) is mass- or volume-limited. This dictates whether to consider the

[1]Copper is the most toxic component of brass, and the National Water Quality Standards are less than 14 μg/L. Water criteria and discharge standards can be found in the EPA and Uniform National Discharge Standards literature; also see <http://www.epa.gov/OST/standards/wqcriteria.html>.)

[2]Deployment effects on the particle size distribution are also an issue when using the particle size characterization results for tests carried out in liquid suspensions to model our gas suspended extinction measurements.

mass- or volume-extinction coefficient. Mass- and volume-extinction coefficients are related to one another by the packing density ρ_p (or the not-necessarily-equivalent quantity, tap density). This quantity is not the same as material (bulk) density, although it does generally scale with bulk density. It also depends on how tightly the material is packed, so that it is not an inherent property of the material but depends on other factors specific to a particular sample, such as compressibility and the particle size distribution.

Deployment conditions may favor or exclude a material. This places some importance on properties that, at first glance, might not seem relevant. Polymers are one example. Polymers have some attractive properties as an obscuration candidate. But, if the deployment heats the sample too much (>300° C), then polymers will melt and cannot be considered. Polymers can be considered, however, for a method that does not heat or compress the material. Consequently, it is desirable to have some indications about the deployment conditions in selecting obscuration material candidates and to test materials under conditions that resemble those for the planned deployment.

Background

The line-of-sight attenuation of incident radiation (I_o) as a function of extinction coefficient $\sigma(\lambda)$, material concentration (c), and pathlength (L) is given by

$$I(\lambda) = I_o(\lambda)\, e^{-\sigma(\lambda)cL}, \tag{1}$$

where I denotes the transmitted intensity. This can be equivalently expressed in the terms of the extinction $E(\lambda)$ as Beer's Law,[3]

$$E(\lambda) = -\log\left(\frac{I_o(\lambda)}{I(\lambda)}\right) = 2.303\sigma(\lambda)cL\ . \tag{2}$$

The quantity cL is the column density, the number of particles per unit area in the line of sight. The extinction coefficient $\sigma(\lambda)$ can be expressed in several ways, depending on how the amount of material (concentration) is specified. In molecular spectroscopy applications, c is often in molar concentration (moles/l) and $\sigma(\lambda)$ is the molar absorption coefficient in representative units (non SI) of l/(mole cm).[4] For particulate samples and obscuration studies, c is often expressed as mass loading (g/m^3), so that the mass-extinction coefficient $\sigma_m(\lambda)$ is in units of m^2/g. Alternatively, the volume-extinction coefficient, $\sigma_v(\lambda)$ in m^2/cc, is obtained when the mass loading is multiplied by the packing density ρ_p, i.e., $\sigma_v(\lambda) = \rho_p\, \sigma_m(\lambda)$.

Mass-extinction coefficients $\sigma_m(\lambda,r)$ depend on the wavelength, particle radius and its complex index of refraction. The extinction coefficient σ_m is the sum of contributions due to scattering σ_{sc} and absorption, σ_{abs}; $\sigma_m = \sigma_{sc} + \sigma_{abs}$. The fraction of overall extinction due to scattering is the albedo,

[3]Extinction $E(\lambda)$ is analogous to absorbance $A(\lambda)$. The term extinction for this quantity is somewhat confusing since it also refers generally to particle-induced light attenuation The analogous term "absorbance" is less problematic since it is different from absorption that causes it.

[4]This is usually applied for liquids. For gases, one case is c in atm and σ in $atm^{-1}cm^{-1}$. Absorption intensity can be expressed in many units and this can be a source of some confusion. Discussions and conversion tables can be found in Rao (1976) and Okabe (1978). Also, using σ for extinction of a macroscopic sample is an unfortunate choice since it is more often used for molecular ($A = n\sigma L$) rather than molar ($A = \varepsilon cL$) coefficients.

$\omega = \sigma_{sc}/(\sigma_{sc} + \sigma_{abs})$. There are several ways to express the extinction parameter. The (dimensionless) extinction efficiency Q_{ext} is the ratio of the extinction cross section ($\sigma_{ext}(\lambda,r)$ in cm^2) to the particle area,

$$Q_{ext} = \frac{\sigma_{ext}(\lambda, r)}{A} . \tag{3}$$

The mass-extinction coefficient is the extinction cross section divided by the mass of the particle,

$$\sigma_m(\lambda, r) = \frac{\sigma_{ext}(\lambda, r)}{\rho V} , \tag{4}$$

where ρ is the bulk material density, so that for spherical particles, Q_{ext} is related to $\sigma_m(\lambda,r)$

$$\sigma_m(\lambda, r) = \frac{1.5 Q_{ext}(\lambda, r)}{\rho d} , \tag{5}$$

where d denotes the spherical particle diameter. Powders are commonly polydisperse, and the cumulative mass-extinction coefficient is given by an average over the particle size distribution by mass n_m,[5]

$$\sigma_m(\lambda) = \frac{\int \sigma_m(\lambda, r) n_m(r) dr}{\int n_m(r) dr} . \tag{6}$$

As stated above, the extinction coefficient is the sum of scattering and absorption contributions. It depends on the complex index of refraction m, $m = n + ik$. m is composed of a real part n, which is related to scattering, and an imaginary part k, which governs absorption. Extinction also depends upon the ratio of particle size to the wavelength of incident radiation. If $r/\lambda << 1$ and the index of refraction is complex ($k \neq 0$), then extinction is dominated by absorption. The absorption coefficient is given by $\alpha = 4\pi k/\lambda$. The wavelength dependence of extinction is primarily determined by scattering when $n >> k$.

Extinction is often described in terms of a reduced variable, the size parameter $x = 2\pi r/\lambda$, or a similar quantity that includes the (modulus of the) index of refraction, the phase shift, $\rho = 2x = 4\pi r(m - 1)/\lambda$.[6] The scattering depends on the particle size and the real part of the index of refraction. The imaginary part reflects absorption and affects the extinction magnitude. The size dependence can be determined either by an explicit Mie scattering calculation or estimated by an analytical equation that approximates the exact Mie theory. In the latter approach, the scattering efficiency Q_{ext} can be expressed for nonabsorbing spheres in a general and convenient way using the extinction equation (van de Hulst, 1983, p. 176),

$$Q_{ext} = 2 - \frac{4 \sin\rho}{\rho} + \frac{4(1 - \cos\rho)}{\rho^2} . \tag{7}$$

[5]Appendix A provides more discussion on distribution-averaged extinction coefficients.

[6]For particles dispersed in a liquid, $m = m_1/m_2$, where m_1 is the index of the particle and m_2 is of the liquid (and $\lambda = \lambda_{vac}/m_2$).

This solution to the scattering problem is less appropriate for high m (m > 2). Among other approximations, dispersion and absorption are neglected (i.e., m is constant, k = 0, and m = n). This expression exhibits the correct behavior in the limits of small ρ (Rayleigh-like) and large ρ (physical optics, $Q_{ext} = 2$). A plot of this curve is shown in Fig. 1. The benefit of having an analytical although approximate solution to extinction may be more easily appreciated by using results for specific examples. Mass-extinction curves for various n, λ, and d are plotted in Fig. 2. The curves are plots of Eq. (7), which are similar to those of Fig. 1 except with the axes converted. σ_m is calculated from Q_{ext} using Eq. (5) with an arbitrarily chosen density of 2. The mass-extinction curves are shown as a function of particle diameter (or wavelength in the inset) by converting ρ to d, $d = \rho\lambda/(2\pi(m - 1))$, which requires specifying m and λ (or to λ, where $\lambda = 2\pi d(m - 1)/\rho$, specifying m and d).

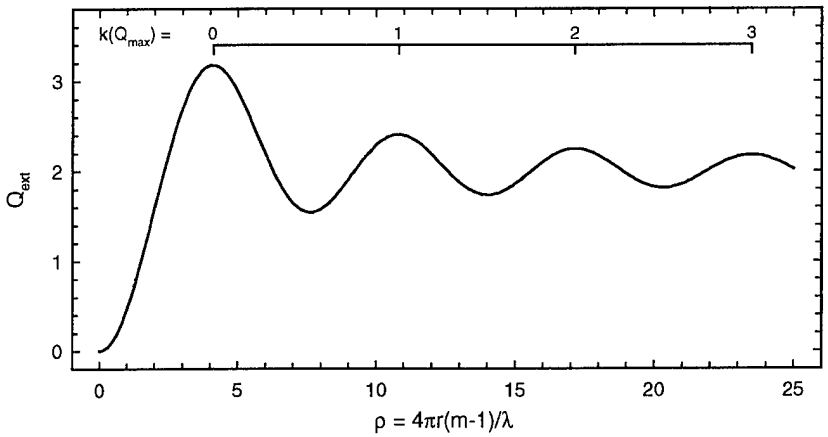

Fig. 1 – The extinction curve, Eq. (7)

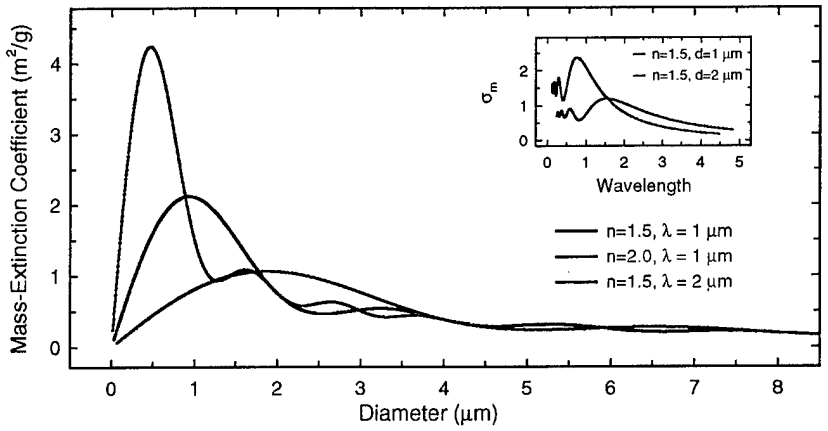

Fig. 2 – Mass-extinction curve (σ_m) derived from the extinction curve (Eq. (7) and Fig. 1) as a function of particle diameter for several values of refractive index and wavelength. Inset: mass extinction as a function of wavelength for two particle diameters. A particle bulk density of 2 was assumed in all cases.

The maxima of the extinction curve in Fig. 1 are given by

$$\rho_k(Q_{max}) = \left(k + \frac{3}{4}\right)2\pi \quad , \tag{8}$$

where k = 0,1,2,... correspond to maxima in Q_{ext} with increasing ρ. This result is based on the first two terms of Eq. (7); this approximation is within 10% of the three-term result for the first peak and improves for larger ρ (i.e., for k > 0). The first and largest peak corresponds to $\rho_0 = 4.712 = 4\pi r(m - 1)/\lambda$. Solving this for the particle radius or diameter provides a convenient way to calculate the particle size for the highest extinction at a particular wavelength and for a specific real index of refraction,

$$d = \frac{0.75\lambda}{m - 1} \quad . \tag{9}$$

Estimates for the particle diameter that result in the maximum Q agree closely with results from the rigorous Mie theory calculations. Table 1 and Fig. 3 illustrate some results for $d(Q_{max})/\lambda$ and $d(\lambda(Q_{max}))$ for several values of m. d/λ falls in the 2 (for m = 1.4) to 0.33 (for m = 3.3) range. For wavelengths in the 3-12 μm range, the approximate solution indicates that the range of particle sizes for Q_{max} are 1-20 mm.

Table 1 – Particle Diameters for Q_{max} for Selected Values of m

m =	1.4	1.8	2.2	3.3
$d(Q_{max})/\lambda$	1.9	0.94	0.62	0.33
$d(Q_{max})$ at 4 μm	7.5	1.9	2.5	1.3
$d(Q_{max})$ at 10 μm	19	9.3	6.2	3.3

This analytical form for the extinction provides a reliable estimate of the value of Q_{max} only in the absence of absorption and for m < 2. Equation (7) implies that the value of Q_{max} depends only on $\rho(Q_{max})$, i.e., that it is the same for homologous extinction curves, which are those with the same d/λ for different λ (and d). But, Q is sensitive not only to d/λ, but also to the values of d and λ. In our size regime, Q_{max} generally decreases with λ for a constant ρ. The analytical expression for extinction provides a convenient method to estimate the average particle size for optimum extinction of various materials. First, this provides a simple way to estimate the average particle size for a powder that will yield high extinction. Second, it was used to analyze measured ultraviolet/visible (uv/vis) transmission spectra for materials in liquid (typically aqueous) suspension as a way to obtain a crude in-house estimate of the average particle size for several samples.

In cases where the indices of refraction are available, Mie theory calculations provide a more rigorous determination of the extinction for spherical particles. A Fortran routine for these calculations was previously developed in our laboratory (Ladouceur et al., 1997; the code is based on routines from Dave (1968)). This program computes the scattering and absorption cross sections using Mie theory from the input complex index of refraction, particle size, and wavelength. Direct-transmission losses are determined with a radiation-transport model assuming single scattering. The routine can provide phase functions, scattering asymmetry, and other quantities concerning the interaction of particles and light, but our primary concern in this work is the extinction coefficient.

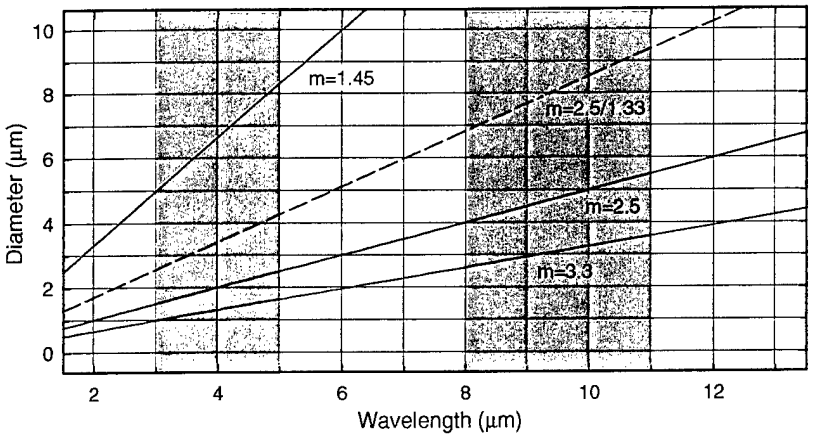

Fig. 3 – Plot of particle diameters that yield maximum extinction as a function of wavelength for several values of m based on the approximate solution (Eq. (9)) to the extinction curve. The values of m are close to those for the materials investigated: m = 1.45, salts; m = 2,5, silicon carbide, iron oxide, and titanium oxide; m = 3,3, graphite. The dashed line indicates results for aqueous suspension (in which case the wavelength axis should be taken as λ/m_2, where m_2 is the index of the liquid – 1.33 for water).

Absorption affects the extinction curves in several ways. The spectral dependence of Q is mostly dictated by n, but as the particles become small ($r/\lambda << 1$ in the Rayleigh limit), Q decreases rapidly in the nonabsorbing case but it remains quite high and is nearly particle-size independent for absorbing particles. Very small particles behave similarly to an absorbing gas if scattering is negligible, and the penetration depth is much less than the particle size. (Appendix B addresses the prospects for strongly absorbing gases as obscurants.) Under these circumstances, the extinction is due almost entirely to absorption; it depends on the column density, and the particle size or shape has little effect. Broad absorptions, such as for metals and semimetals generally increase Q_{ext} relative to what it would be for nonabsorbing particles with the same n. Under some circumstances, narrow absorptions reduce the extinction, specifically (for r/λ near 1) on the short wavelength side of the resonance (van der Hulst, 1983, p. 193). (This is the case for small particles with small to moderate ρ and affects a broader region for larger particles.) The resonance decreases the real part of the index and reduces the scattering more than the absorption increases. Absorption also lowers the albedo and decreases the amount of in-scattering (and the need to incorporate a formalism to account for it, such as with a two-flux model).

Methods

Our approach to finding a suitable infrared obscuring material is to initially select those expected to have promising extinction and then to evaluate them by measuring the extinction coefficient in both spectral bands. Materials were initially chosen because they exhibited promising extinction (graphite: Hartman, 1995, and Hoock and Sutherland, 1993) or because they absorb in or near the 3-5 or 8-12 μm regions. Absorptions were identified by the material optical constants (Palik, 1984, for silica, titania, and silicon carbide); Hoock and Sutherland, 1993 for graphite, calcium carbonate) or from infrared spectra of bulk inorganic compounds (Nyquist and Kagel, 1971). The latter indicate that carbonate and phosphate salts have strong absorptions in the 8-12 μm band. One of the few classes of compounds with strong absorptions in the 3-5 μm band is ammonium-containing salts. (Compounds with N-H bonds exhibit absorptions near 3 μm, but many of these are weak, such as for ammonia, NH_3; ammonium, NH_4^+, on the

other hand, has a relatively strong absorption.) Powders were procured with particle sizes close to those predicted to yield high extinction as indicated by Eq. (9). Many samples were characterized by particle-size distribution analysis. The measured size distribution provides a way to gauge how close that sample is to the optimal size for extinction. On this basis, the measured extinction can roughly be extrapolated to the best-case particle size to determine whether that material has potential for providing adequate extinction. Field tests were carried out to investigate how different kinds of materials would deploy and to attempt to corroborate that the extinction realized in the field was consistent with the coefficients measured in the laboratory.

EXPERIMENTAL

Spectral transmission in the 200-900 nm region was measured for aqueous suspensions for some powders to estimate the average particle size. Sample concentrations were adjusted to yield absorbances in the 0.5-1.0 OD range. The data were collected using a 1-cm pathlength dip probe and a portable Spectral Instruments fiber optic coupled CCD spectrometer (Spectral Instruments 410).

Extinction measurements for dry powders were performed on the apparatus constructed at NRL (Ladouceur et al., 1997). The instrument has been described previously and will only be discussed briefly. A schematic diagram of the apparatus is shown in Fig. 4. It consists of an aerosol flow tube that serves as the sample compartment for a Fourier transform infrared spectrometer (FTIR, Mattson Instruments, Cygnus 100) operating with an external detector. Powder is manually placed in the groove of a rotating platen equipped with a scraper, which controls the powder height in the groove and consequently the mass loading. The powder is introduced to the tube by a venturi nozzle (Air-Vac Engineering Co., Inc. model TD110H). It is mixed with a nitrogen gas flow directed up the tube (total flow = 42.5 LPM). The flow tube is 87-cm long and has an 11.4-cm inner diameter. It has two purged

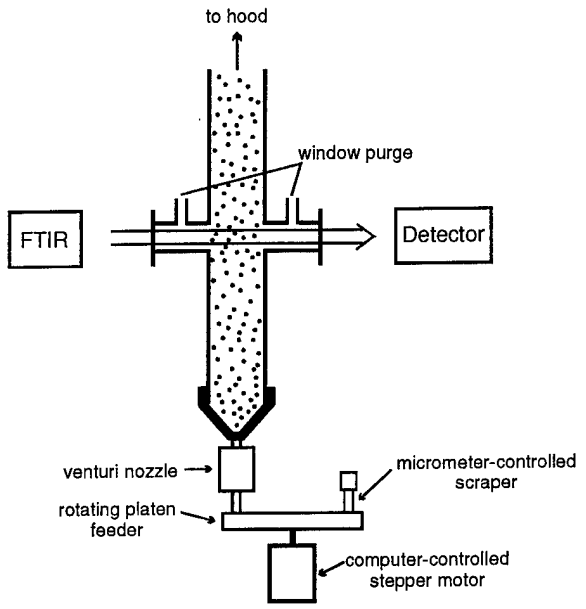

Fig. 4 – Schematic diagram of the apparatus used to measure extinction coefficients in this work

sidearms 35 cm above the funnel, which are used to attach NaCl windows (13 cm from the tube) for the IR beam of the FTIR to intersect the entrained powder. Spectra are recorded in single-beam mode in the 500-4000 cm^{-1} range; they are typically collected with 4 cm^{-1} resolution by averaging 16 scans. The absorbance is obtained using a background scan taken before the powder is fed into the apparatus. A scan after the run is also taken to avoid interferences from material deposited on the window or other residual transmission changes. Measurements are performed using 2-8 g of material, which is taken up in 0.5-2.0 minutes (20-80 L); the typical range of mass loading is 40-120 g/m^3. Previous work demonstrated that the mass-extinction coefficients measured were not strongly affected by the mass loading within this range.

Powders were used as received from Aldrich Chemical Company (1-2 μm synthetic graphite, catalog no. 28286-3), Ferro Colors (iron oxide, F-6331), ChemGuard (monoammononium hydrogen phosphate, Phos-Chek®P/30), Electroabrasives (silicon carbide, 800 and 1200-W), and Alfa Aesar (natural graphite -325 mesh, 40798; sodium ammonium hydrogen phosphate, 40320; ammonium hydrogen carbonate, 14249; calcium carbonate, 12365; glassy carbon spheres, 0.4-12 μm, 38004).

LABORATORY RESULTS

Particle Size Measurements

The particle size distribution was characterized for many of the samples. Table 2 is a summary of the results. Information about the size distribution was obtained from several sources. The manufacturers provide specifications for some powders. In a few cases, we roughly estimated the average particle size based on the uv/vis transmission of liquid suspensions of the powder. Analyses that provided detailed size distributions by particle number and mass/volume were obtained from commercial particle sizing laboratories, Micromeritics, Inc., and Particle Characterization Laboratories.

The distribution-averaged mass-extinction coefficient $\langle\sigma_m\rangle_n$ can be calculated using Eq. (3). This is expressed in terms of particle size distribution by mass, $n_m(r)$. The distribution can also be given by number of particles for each size. A number distribution n(r) can be converted to $n_m(r)$ by multiplying each probability element of the former by the particle mass for that size, [7] i.e., by $\rho(4/3)\pi r^3$ (or for volume distribution $n_v(r)$, by $(4/3)\pi r^3$). The mean radius is larger for the mass distribution, and the difference is greater for broader distributions (see Appendix A).

The size distribution can be used to assess how close the sample is to the optimum size for extinction. If the size-dependent extinction cross sections are known, it can be used to calculate the distribution-averaged extinction coefficient $\langle\sigma_m\rangle$. There are many ways to express extinction for a particle or collection of particles and for particle distributions, so there are different approaches to $\langle\sigma_m\rangle$. The most straightforward is to calculate the cumulative extinction (in area) for a collection of particles and divide it by the total mass. This is expressed in Eq. (3) using the mass-extinction coefficient and mass probability. Equivalently, the cross section and number probability can be used to calculate the extinction for each element in the numerator (see Appendix A).

[7] Distributions by volume ($n_v(r)$) and by mass ($n_m(r)$) have the same radial dependence; they are related by the bulk material density, which is independent of the radius. These will have the distribution parameters: mean radius, fullwidth, etc. The particle number distribution (n(r)), however, has a different power dependence on the radius; $n_m(r) \propto (n(r))r^3$.

Table 2 – Results of Particle Size Analyses for Powders

Material	Methods†	Particle Distribution (μm)			Mass/Volume Distribution (μm)		
		Mean	10% less than	90% less than	Mean	10% less than	90% less than
Brass	1	0.21	0.11	0.36	4.00	0.60	8.38
	2				1.44	0.62	3.30
Graphite (1-2 μm)	1	1.1	0.46	2.1	6.7	1.8	12
	3	1.15	0.43	1.9	2.8	1.2	4.8
Graphite (-325 mesh)	1	2.8	1.6	4.5	30	4.9	64
Glassy carbon spheres	1	5.0	2.5	8.1	7.7	4.5	10.6
Silicon carbide 800	4a	9	Range: 3-20				
Silicon carbide 1200	4a	3	Range: 0-11				
Boron nitride	4b				10.6 (median)		
	1	0.80	0.5	0.95	3.0	0.7	9.1
Monammonium phosphate	1	1.7	0.75	3.3	16.5	4.6	34.6
	4c	30 (median)	16	48			
Iron oxide	1	0.80	0.60	1.1	4.0	0.7	8.7
	3				14.5	13.9	15.1
Titanium oxide	2	0.31	0.16	0.83	0.76	0.24	0.85

†Particle sizing methods: 1. Micromeritics, Elzone™ method 2. Micromeritics, Sedisperse™ method 3. Particle Characterization Laboratories using light scattering 4. Manufacturer specified: 4a. Electroabrasives; 4b. Carborundum; 4c: ChemGuard.

An in-house method was used to estimate the average particle size of powders in aqueous suspensions using uv/vis transmission. The wavelength corresponding to the peak absorbance was used to determine the average particle size using Eq. (9), where the index of the material is divided by the index of the liquid (1.33 for water). The method was initially tested successfully on monodisperse 0.99-μm polystryrene spheres (n = 1.58, $\lambda(E_{max})$ = 0.32 nm). This method also yielded reasonable results for SiO_2 (Zeothix 77, 4 μm) and for TiO_2 (Fluka, 0.4 μm). Other samples tested (e.g., graphite, silicon carbide, iron black) have larger particles so that the extinction maximum occurs at longer wavelength (near IR or mid-IR) than the uv/vis and could not be determined in this manner. This method provides only an estimate of the average particle size and does not characterize the distribution, the details of which are important to realistically estimate a sample's extinction. This transmission method has several possible drawbacks. (1) It uses a liquid suspension so that the particle distribution observed could be different from the gas suspension in the flow tube and from the planned deployment. The Micromeritics Elzone method also uses a liquid suspension, so if there is a medium dispersion problem it would also adversely affect the more thorough

analyses. (2) The average size measured optically in a liquid is different than what it would be for the same distribution in a different medium (gas). This problem would be reduced by accounting for the liquid index dispersion with wavelength.

Particle-size distribution analyses were performed for the two samples of graphite (2 μm and -325 mesh), glassy carbon spheres, monoammonium phosphate (MAP), and iron oxide. Results from previous studies, including titanium oxide, brass, and boron nitride, are included for completeness. The results are listed for the mass/volume as well as particle number distributions. A large ratio of the mass/volume-to-particle number mean particle size indicates a wide distribution, such as for graphite (-325) and MAP. In this case, much of the mass is taken up by the relatively few larger particles that contribute less to the extinction. Graphite (2 μm) and the carbon spheres have relatively narrow distributions. The size distribution for graphite (2 μm) was corroborated by other observations. The highest extinction in the flow-tube spectrum was at 6 μm and this correlates with λ from Q_{max} as given by Eq. (9). In addition, the extinction spectrum agrees with a spectrum calculated from a distribution-weighted sum of extinction curves for discrete particle sizes as described below.

Measured Extinction Coefficients for Obscurant Candidates

The mass-extinction coefficient is determined from the measured absorbance A, the mass loading M_L, and the pathlength L by

$$\sigma_m = \frac{2.303A}{M_L L}, \tag{10}$$

where the factor 2.303 converts absorbance from common log to natural log for the calculation of σ_m (which is defined as a natural log). L is the flow-tube diameter, and M_L is the mass loading, which is mass of the sample divided by total volume flowed. Absorbance curves measured over the 2-13 μm range were converted to mass-extinction curves using Eq. (10) as shown in Figs. 5 and 6. Table 3 lists band-averaged mass-extinction coefficients for all of the materials measured in descending order of mass extinction in the 3-5 μm band. The table also includes packing densities for the powders. Results from previous work on brass,[8] boron nitride, and boric acid are included for comparison (Ladouceur et al., 1997).

The results listed in Table 3 for both the 3-5 and 8-12 μm bands are band-averaged mass-extinction coefficients. In our previous IR obscurants work, the results for each band were presented in terms of a specific obscuration example using a 350 K blackbody and 70 cm^3 of material dispersed into a 10-m diameter cloud. For many of the materials tested in this work, the extinction does not vary much with wavelength, especially within one of the spectral bands of interest. Consequently, the effect of weighting by the blackbody spectrum is minimal; a simple band average and one that specifically accounts for the blackbody emission yield similar results for the extinction. The biggest differences are for the salts, which have structured extinction, and silicon carbide, which has structure in the long wavelength band.[9]

[8]The coefficients for brass have recently been revised (Ladouceur et al., 1998) to about four times higher than those originally reported (Ladouceur et al., 1997).

[9]The difference in blackbody radiation between 350 K and 300 K is related to the extinction (contrast) needed for obscuration. The ratio of emission within the bands for 350 K/300 K is 2.1 for 8-12 μm and 5.1 for 3-5 μm. (The ratio of emission in the 8-12 μm band to that in the 3-5 μm band is 1.72 at 350 K and 4.2 at 300 K.)

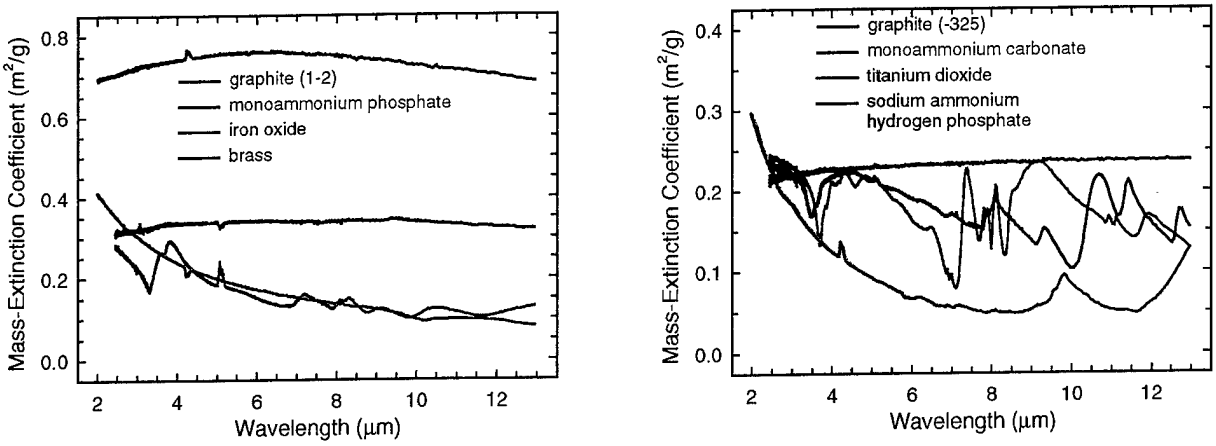

Fig. 5 – Mass-extinction coefficients measured for (left panel) graphite (2 μm), MAP, iron oxide, and brass; (right panel) graphite (-325), monoammonium carbonate, titanium dioxide, and sodium ammonium hydrogen phosphate

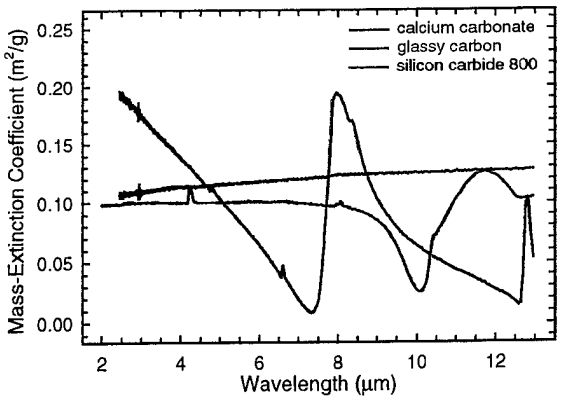

Fig. 6 – Mass-extinction coefficients measured for calcium carbonate, silicon carbide, and glassy carbon

Table 3– Measured Extinction Coefficients and Packing Densities

Material	Mass Extinction Coefficient (m^2/g)		Volume Extinction Coefficient (m^2/cc)		Packing Density (g/cc)
	3-5 μm	8-12 μm	3-5 μm	8-12 μm	
Graphite (1-2)	0.74	0.73	0.29	0.28	0.39
Brass[a]	0.34	0.33	0.51	0.49	1.5
Iron black	0.24	0.11	0.16	0.08	0.67
Graphite (-325 mesh)	0.23	0.24	0.17	0.18	0.74
Monoammonium hydrogen phosphate	0.22	0.11	0.27	0.14	1.2
Sodium ammonium hydrogen phosphate	0.21	0.16	0.24	0.18	1.14
Ammonium hydrogen carbonate	0.20	0.17	0.18	0.15	0.9
Titanium oxide	0.13	0.06	0.16	0.07	1.2
Calcium carbonate	0.12	0.05	0.09	0.04	0.79
Silicon carbide 1200 mesh	0.12	0.07	0.14	0.08	1.12
Glassy carbon spheres	0.11	0.13	0.09	0.1	0.79
Silicon carbide 800 mesh	0.10	0.08	0.13	0.11	1.35
Boron nitride[b]	0.07	0.05	0.05	0.03	0.67
Boric acid[b]	0.02	0.01	0.01	0.01	0.67

[a] Ladouceur et al., 1998.
[b] Ladouceur et al., 1997.

Several materials did not flow up the tube and their extinction coefficients were not measured. This includes some polymer samples, specifically polypropylene, polyethylene glycol, and PVC. The first two are listed by the manufacturer (Micropowders) to have average particle sizes <25 μm, which may account for the difficulty in getting them entrained. (Particle size limitations on lifting in a gas stream have been discussed previously in Ladouceur et al. (1998)). In addition, a small particle diameter sample of SiO_2 (Zeothix 77, nominal 4-μm diameter) failed to be carried up. The same result was found for other relatively small particle size samples (<10 μm), such as AlO_2, CuO, and SnO.

DISCUSSION

The primary result of our study is that the 2-μm graphite sample exhibits the highest mass-extinction coefficient (0.74 and 0.73 m^2/g in the 3-5 and 8-12 μm bands, respectively) of the materials tested. This is twice as high as the material with the next highest σ_m, which is brass. Others with high σ_m in the 3-5 μm band are iron black, phosphate salts, and graphite (-325). Of these, the coefficient for the longer band is lower for iron black and the phosphates. The result that σ_m for graphite is twice as high as for brass is similar to what has been previously reported (Edwards et al., 1992). In those cases, the sizes and

shapes were somewhat different, and substantially higher σ_m were reported. The higher σ_m found in the previous reports is likely due to the different method of deployment. Our method of entraining the powder is relatively gentle, so that we may be subject to aggregation, and the larger realized particle sizes reduce the extinction. In the other studies, the powders were more vigorously dispersed. The particles are probably broken apart to a greater extent and would more closely approach the primary particle size, resulting in higher measured extinction coefficients.

The volume-extinction coefficient σ_v is the product of σ_m and ρ. It is well known that due to its high packing density, brass has a higher σ_v (at 0.51 and 0.49 m^2/cc) than graphite. ρ for brass is almost four times that of 2-μm graphite, and it is lower for 2-μm graphite than for any of the other materials tested. The phosphates (MAP and SAHP) and even graphite (-325) have relatively high packing densities, so that their measured values for σ_v are closer to those for the smaller graphite. The value measured for TiO_2 is consistent with the one calculated in the 3-5-μm band from the absorbance spectrum and mass loading previously reported (Ladouceur et al., 1999).

Some trends in the extinction coefficients were expected. First of all, similar to the bulk spectra, the carbonate and phosphate salts exhibit the most spectral variation. The resonances are stronger for the carbonate salts, but the band-averaged extinction is stronger for the phosphate salts. In some cases, the resonance effect of decreasing the real part of the index and thus the extinction on the low wavelength side is evident. The decrease for silicon carbide at 10 μm (and then the increase at 11.5 μm) is a clear example. The observed spectrum agrees with Mie calculations in this respect (Appendix C).

As mentioned above, the 2-μm graphite spectrum peaks at 6 μm, and this is close to what is predicted for Q_{max} from Eq. (9) and Table 1. Mie calculations were performed for graphite to obtain mass-extinction coefficients in the infrared for various particle sizes (0.5,1,2,..10 μm) as shown in Fig. 7. Optical constants for graphite were obtained from Hoock, Jr. and Sutherland (1993). The peak wavelength (λ_{max}) is approximately linear with particle diameter, and d/λ_{max} is close to 1/3. Also, the product of the maximum $\sigma_m(\lambda_{max})$ and the diameter is about 2-2.5 in each case. (This is because Q_{max} is nearly constant and $Q_{max} \propto \sigma_m d$.) By inspection, the extinction we measure for the 2-μm graphite is similar to the curve for the 3-μm diameter particle. A distribution-averaged extinction spectrum was calculated in which a Gaussian mass distribution was adjusted to agree with the observed extinction spectrum. The results are shown in Fig. 7. The resulting mass distribution (mean = 2.4 μm, full-width = 1 μm), shown in the inset of the figure, is similar to the distribution from the particle size characterizations. The agreement is better with the PCL results (2.8-μm mean) than with those from Micromeritics (6.7-μm mean). Unlike the observed spectrum, the calculated one falls off at longer wavelength, which may indicate some particles at higher mass, a bimodal distribution. This could be from clumping in our measurement.

The trend in the extinction as a function of particle size follows the expected result in the cases where the same materials with different average particle sizes were measured. Two samples of both graphite and silicon carbide were tested. In each case, the sample with the smaller average particle size yielded the higher extinction, and it is at or larger than the optimum (based on the extinction equation and the plot in Fig. 3 of radius for Q_{max}). The 3-μm average diameter silicon carbide 1200 yields a slightly higher σ_m than its larger counterpart. For graphite, it is useful to consider the size dependence using the results for the Mie scattering calculations shown in Fig. 7. The measured σ_m for the 2-μm sample indicates that the particles are slightly larger than the optimum (about 1.5 μm) for the 3-5 μm band. σ_m for the larger graphite is higher than might be expected based on the particle size analyses and the Mie scattering calculations. The measured σ_m ratio is about the 3:1 ratio, favoring the smaller sample in both bands. If

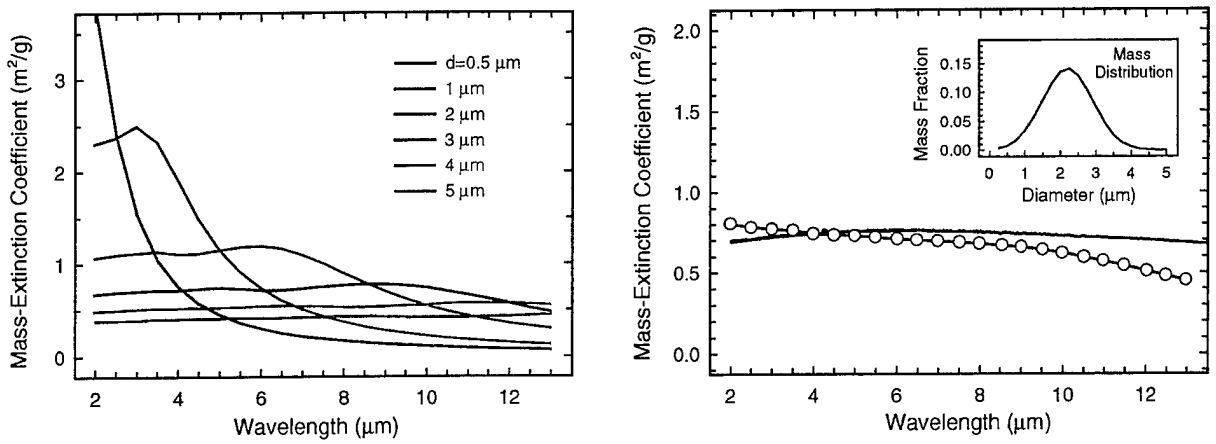

Fig. 7 – (Left panel) Calculated $\sigma_m(\lambda)$ for graphite as a function of wavelength for several particle diameters; (right panel) calculated mass-extinction spectrum for graphite (blue line with symbols) using size-specific $\sigma_m(\lambda)$ from the left panel and the size distribution shown in the inset. The observed $\sigma_m(\lambda)$ is the black solid line.

we apply the very approximate result from above in which the product $\sigma_m d$ is constant, then this implies that the ratio of sizes is inversely proportional to the ratio of σ_m and that the larger graphite is about 3 times larger. This ratio of sizes inferred from the relative extinction coefficients is somewhat smaller than the one from the particle characterization sizes. The ratio of mean diameters from the characterization results are 4.5 (using Micromeritics for the smaller sample) or 11 (using the PCL result, which agrees more closely with the measured extinction for the smaller graphite sample). The trend is correct. More quantitative agreement may be achieved by a more rigorous calculation that includes the distribution and spectral variation of the optical constants.

The particle size results in Table 2 and the calculated optimum particle size ($d(Q_{max})$, such as in Fig. 3 and Table 1) can be used to estimate how close the measured values are to those calculated to be optimal for that material. The measured σ_m depends on the mean particle size, which can be considered how close it is to that calculated for Q_{max}, and the width of the distribution. An indication of the latter is the 10% and 90% sizes and how much larger the mass/volume mean is than the number mean. The mean size for 2-μm graphite is close to its d_{max}, and the distribution appears to be narrow compared to the other materials. The larger graphite has a number mean size that should yield high extinction for the longer wavelength band, but the distribution appears to be quite broad. For the materials with n close to 2.5 (TiO_2, SiC, FeO), for wavelengths of 4 and 10 μm (in the middle of each band), d_{max} is approximately 2 and 5 μm. Unfortunately, there are some discrepancies in the results for the particle sizes analyses. Based on the PCL result, the iron oxide sample has a larger particle size than the one calculated for high extinction, so that significant improvement may result from finding this material with smaller particles. (The PCL distribution is also very narrow.) However, if the sample is actually closer to the considerably smaller average size reported by Micromeritics, the measured extinction is not far from the best that one can expect for iron oxide. Similarly, based on the specifications from the manufacturer, there is considerable room for improvement in the MAP. The Micromeritics sizing results indicate that the particles are smaller, but with a broad distribution. This material is partially soluble in the solvent (methanol) used for the analysis, and this may have affected the measured size distribution.

Mie calculations of the extinction coefficients were carried out as a function of particle size and wavelength for several materials, specifically those for which the wavelength-dependent indices of refraction could be found. These calculations provide a better determination of the coefficients than the analytical approximation. In addition to graphite (Fig. 7), calculations were performed for silicon oxide

(SiO_2), aluminum oxide (Al_2O_3), silicon carbide (SiC), and iron oxide (Fe_xO_y). The results are plotted in Appendix C for all except the last of these, which is shown in Fig. 8. The most promising of these materials is iron oxide. The peak σ_m at a wavelength of 3 μm for a 1-μm diameter particle is 3.4 m^2/g; in the 8-12 μm band, it is about 0.7 m^2/g for 2-μm particles. A sample with particle sizes close to these values should yield a respectable extinction. Also, this material is not toxic. The other materials calculated were not as promising, except for the long wavelength band for silica. The extinction was generally low for the oxides. As described above, the SiC extinction almost vanishes in the middle of the long wavelength band due to the absorption band effect on the real part of the complex index of refraction, which reduces the scattering.

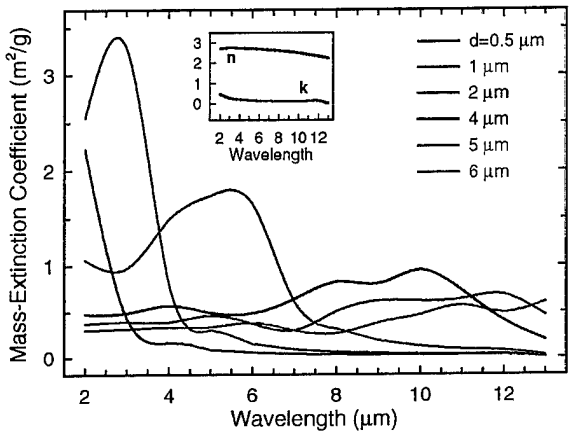

Fig. 8 – Calculated mass-extinction coefficients as a function of wavelength for several particle diameters for iron oxide

There are several ways to improve the extinction of a material, but their effectiveness may depend on the planned application. For example, increasing the packing density can improve the volume-extinction coefficient (for a volume-limited payload) but it will not help if the application is mass-limited. It is therefore worth considering whether a payload is mass- or volume-limited or both in comparing the extinction potential of various materials. Consider the extinction for brass and graphite for deployment in a planned delivery system. If the mass (M_L) and volume (V_L) limitations are known, they can be used to specify an effective "limitations density" ρ_L (defined as $\rho_L = M_L/V_L$) to determine the conditions under which each material is mass- or volume-limited. It is mass-limited when $\rho_L < \rho_p$ and volume-limited when the opposite is true. ρ_p (graphite) = 0.4 g/ml and ρ_p (brass) = 1.5 g/ml, so that for ρ_L in between these, brass is mass-limited and graphite is volume-limited. Since σ_m (graphite) = $2\sigma_m$ (brass), the extinction will be nearly equal for twice the weight of brass. This would occur for ρ_L = 0.8g/ml, i.e., if the constraints were 1 liter for each 0.8 kg, whichever is higher. The mass limit would be reached for brass (with a volume of 0.54 l), and the volume-limited mass for graphite would be 0.4 kg, resulting in the mass ratio of 2. For $\rho_L > 0.8$ and $\rho_L < 0.8$, the extinction is higher with brass and with graphite, respectively. Graphite provides a better combined obscuration figure of merit when its much lower toxicity is considered.

FIELD MEASUREMENTS

Field measurements of the obscuration were conducted at Army Research Laboratory, Blossom Point Site, Maryland. These were primarily intended as a function test for the screen cartridges. Gas grenades are being used to assess the obscuration of the materials in the field and may also serve as an interim deployment mechanism while the vertically launched vehicle is being designed, constructed, and implemented. The screen cartridge design has been described previously (Mills et al., 1998; Veracka, 1999, Ladouceur et al., 1999). Briefly, the 77 ml volume (V_{sc}) screen cartridges use a nitrocellulose detonator to penetrate the membrane of the payload chamber and expel the charge. The cartridges were placed 4 ft from the ground. Sixteen rounds containing nine materials were fired (Table 4). An attempt to collect samples of the dispersed material using 5-cm diameter petri dishes arranged near the detonation area was not successful. (Others have done this before, such as Farrow et al., (1994).)

Table 4 – Materials Used in Extinction Field Test

Material	Number of Rounds	Average Mass Per Cartridge[a] (g)
Brass	3	95
Graphite (2 mic)	3	25
Silica	3	5.7
MAP	2	67
Silicon carbide	1	87
Titanium oxide	1	77
Iron oxide	1	43
Polyethylene glycol	1	43
Polypropylene	1	33

[a] Packed under 200 lb/in.^{2} (Veracka, 1999); this provides an estimate of the packing density for these materials

All of the cartridges fired, and in this respect, the field test was a success. The extinction was measured using blackbody sources monitored with short and long wavelength cameras. Plots of the relative blackbody transmission for the long band for two brass and one graphite cloud are shown in Fig. 9. (In each case, the round was fired between 0.5 and 1 second after the measurement was started.) For the first few seconds after detonation, the clouds were optically thick for almost all of the materials tested. The high extinction demonstrated by the transmission curves for graphite and brass (brass 1) in Fig. 9 is consistent with calculations described below. It also means that quantitative comparisons of the material extinction is not possible based on the results of this test. The duration of the optically thick clouds might have provided some indication of the relative extinction for the samples except that the wind strongly affected how long the clouds persisted. (This may be, however, a realistic test under conditions similar to those expected for the actual deployment.) One of the brass cloud transmission curves (brass 2 in Fig. 9) demonstrates the strong influence of the wind. At first, the wind blew the cloud out of the line of sight of the source, which is why the transmission does not go to zero, and then brought it back again. The transmission is lower at 4 s than right after the round is fired. Several clouds were similarly affected. The graphite clouds were the most persistent (2-10 s) and the titanium oxide clouds were among the least persistent.

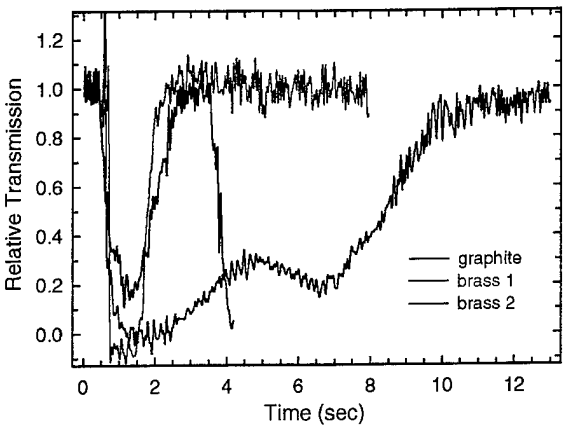

Fig. 9 – Field test results of relative long wavelength blackbody transmission following the generation of obscurant clouds of graphite and brass

It was determined that the extinction for silica is lower than the other materials since it was the only one for which the cloud was not optically thick. Also, several polymers were tested and these were unable to withstand the conditions of the grenade and melted into threads of plastic. This indicates that for applications such as the screen cartridge, polymers cannot be used. (It should be noted that, although they melted, the polymer rounds yielded extinction that was higher than silica and lasted longer than titanium oxide.) But if the ultimate deployment does not involve such a high temperature as the screen cartridge, then polymer powders may remain intact and should not be excluded as candidate materials based on its melting under the harsher conditions of the screen cartridge. Polymers have many advantages as a possible obscurant. Their composition can be varied to tailor the optical constants, and they can often be procured in a very narrow size distribution. Furthermore, these results demonstrate differences between deployment in the field and in the laboratory. The silica sample was not lifted up the flow tube, but it formed a nice cloud in the field tests. The polymers also were not carried up in the laboratory, but they were not melted as in the field test. It would be useful to develop a laboratory apparatus in which the material was dropped instead of lifted to more closely resemble the actual deployment.

The line-of-sight extinction through the cloud depends on its size, the amount of material, and its volume-extinction coefficient. The cloud diameter D and height H are estimated to be 4 m and 1.3 m, respectively. The mass loading is $M_L = \rho_p V_{sc}/V_{cl}$, the cloud cylindrical volume is $(\pi HD^2)/4$, and the pathlength is D, so that extinction (in base *e*) can be reduced to give,

$$E(\lambda)=\sigma_m M_L L=\sigma_m\left(\frac{\rho_p V_{sc}}{V_{cl}}\right)L=\frac{9.2\sigma_v V_{sc}}{\pi DH}. \qquad (11)$$

For the values given above, this yields $E = 19\sigma_v$. (An optical density of 2 or 1% transmission corresponds to an extinction of 4.6 and would occur under these conditions for $\sigma_v = 0.24$ m^2/cc.) Based on these calculations, future tests of this kind may benefit from a smaller payload if the same cloud size results. If the extinction is much higher than required, it also means that the material is not being used efficiently.

CONCLUSIONS

We have measured the extinction coefficients for several candidate obscurant materials. The highest mass-extinction coefficient measured is the one for graphite with a nominal 2 μm particle size. Its mass-extinction coefficient is higher than that of brass in both the long and short wavelength spectral regions. It is also less toxic than brass, so that for mass-limited obscuration applications, graphite is superior to brass and should be used instead. Because of its low packing density, graphite has a relatively lower volume-extinction coefficient. It is only about 60% that of brass. There are several ways to approach finding a material with a volume-extinction coefficient comparable to or greater than that of brass. One way is to consider other carbon materials (nongraphitic carbons, acetylene black, carbon nanotubes) where an improvement may more easily be achieved by increasing the packing density rather than the mass-extinction coefficient. Other promising materials were identified. Iron oxide and MAP were measured to have volume-extinction coefficients comparable to graphite. The specific samples do not have the optimal size distribution for extinction in the spectral regions of interest, so it may be possible to improve the extinction by procuring samples with smaller particles. In summary, graphite can replace brass as an effective obscurant for mass-limited applications, and refinements on the iron oxide and MAP materials should result in a suitable obscurant for volume-limited applications. Field test results indicate that substantial extinction is achieved for the screen cartridges for almost all the materials tested. While high extinction is desirable, producing clouds that are optically thick may indicate that the material could be used more efficiently to obscure a larger area.

ACKNOWLEDGMENTS

The authors acknowledge Mike Veracka for stimulating discussions and field test measurements. Tammie Confer, Lorraine Beahm, and Dan Hartman also contributed to the field test effort.

REFERENCES

C.F. Bohren and D.R. Huffman, *Absorption and Scattering of Light by Small Particles* (John Wiley and Sons, New York, NY, 1983).

J.V. Dave, "Subroutines for Computing the Parameters of the Electromagnetic Radiation Scattered by a Sphere," Report No. 320-3237, IBM Palo Alto Scientific Center, Palo Alto, CA, 1968.

S.W. Farrow, J.H. Wheeler, and J.S. Allan, "Smoke and Obscurant Environmental Sampling and Analysis," DPG-FR-94-703, U.S. Army Dugway Proving Ground, UT, November 1994 (AD-B197061).

H. Edwards, A.B. Marshall, A.K. Rowlands, and J.D. Collins, "Fast Bloom VIS/IR Obscurant Screens," Proceedings of the Smoke/Obscurants Symposium XVI, Vol. 2, pp. 515-556, CRDEC-CR-184, Aberdeen Proving Ground, MD, September 1992 (AD B176968).

J.F. Embury, D. Walker, and C.J. Zimmerman, "Screening Smoke Performance of Commercially Available Powders. 2. Visible Screening by Titanium Oxide," ERDEC-TR-168, Edgewood Research and Development and Engineering Center, MD, June 1994 (AD A284072).

Mark V. Haley and Carl W. Kurnas, "Toxicity and Fate Comparison Between Several Brass and Titanium Oxide Powders," ERDEC-TR-094, Edgewood Research and Development and Engineering Center, MD, July 1993 (AD-A270185).

D.J. Hartman, "Smoke and Obscurants Engineering Handbook, Volume II: Materials Characteristics," ERDEC-CR-195. Edgewood Research and Development and Engineering Center, MD, September 1995.

D.W. Hoock, Jr. and R.A. Sutherland, "Obscuration Countermeasures," in *Countermeasure Systems*, Vol. 7, D.H. Pollock, ed., *The Infrared and Electro-Optical Systems Handbook* (SPIE Optical Engineering Press, Ann Arbor, MI, 1993).

H.C. van de Hulst, *Light Scattering by Small Particles* (Dover Publications, Inc., New York, NY, 1983).

H.D. Ladouceur, A.P. Baronavski, and H.H. Nelson, "Boron Nitride (BN) as an Anisotropic IR Obscurant," Proceedings of the Smoke/Obscurants Symposium XX, p. 95, ERDEC-CR-270, Aberdeen Proving Ground, MD, December 1998.

H.D. Ladouceur, A.P. Baronavski, and H.H. Nelson, "Obscurants for Infrared Countermeasures," NRL/FR/6111--97-9878, December 1997.

H.D. Ladouceur, "A Numerical Study of Transport in Dense Water Mist," Joint Meeting of the United States Sections: The Combustion Institute, March, 1999, Washington, DC.

H.D. Ladouceur, T.S. Confer, A.P. Baronavski, C.H. Douglass, J.C. Owrutsky, and H.H. Nelson, "Evaluation of TiO_2 as a Near IR Obscurant for Shipboard Laser Countermeasures," NRL/MR/5710--99-051, December 1999.

T.E. Mills, D.J. Hartmand, W.G. Rouse, and R.J. Malecki, "Development of a Cartridge for Aerosol Dissemination," Proceedings of the Smoke/Obscurants Symposium XX, p. 231, ERDEC-CR-270, Aberdeen Proving Ground, MD, December 1998.

Richard A. Nyquist and Ronald O. Kagel, *Infrared Spectra of Inorganic Compounds (3800-45 cm^{-1})* (Academic Press, San Diego, CA, 1971).

H. Okabe, *Photochemistry of Small Molecules* (John Wiley and Sons, New York, NY, 1978).

Edward D. Palik, ed., *Handbook of Optical Constants of Solids* (Academic Press, New York, NY, 1984).

K.N. Rao, "Infrared Intensities," in *Molecular Spectroscopy: Modern Research*, Vol. 3, K. Narahari Rao and C. Weldon, eds. (New York, Academic Press, 1976).

M. Veracka, "An Initial Investigation of Shipboard Imager Obscuration Technology," NRL/MR/5710--99-8408, October 1999.

Appendix A

DISTRIBUTION-AVERAGED MASS-EXTINCTION COEFFICIENTS

The distribution-averaged mass-extinction coefficient $<\sigma_m>$ for a collection of particles is given by the total extinction divided by the total mass:

$$<\sigma_m> = \frac{\sum \text{extinction}}{\sum \text{mass}} \quad .$$

The extinction for the i^{th} particle with a radius r_i can be expressed as a cross section $\sigma_{ext,i}$ (in units of area), or dividing this by the particle mass m_i, as the mass-weighted cross section or mass-extinction coefficient (in area/mass),

$$\sigma_{m,i} = \frac{\sigma_{ext,i}}{m_i} = \frac{\sigma_{ext,i}}{\rho(4\pi/3)r_i^3} \quad .$$

The distribution can be represented as a number distribution n_i, or if each particle probability is multiplied by its mass, as a mass distribution,

$$n_{m,i} = m_i n_i \quad .$$

The total extinction can be written as the number distribution weighted sum of cross sections or as the mass distribution weighted sum of the mass-extinction coefficients. These are equivalent, and both sums yield a cumulative extinction in units of area (they are equivalent because the mass in σ_m cancels with the one in n_m),

$$\sum \text{extinction} = \sum \sigma_{ext,i} n_i = \sum \sigma_{m,i} n_{m,i} \quad ,$$

so that

$$<\sigma_m> = \frac{\sum \sigma_{ext,i} n_i}{\sum \rho(4\pi/3) r_i^3 n_i} = \frac{\sum \sigma_{m,i} m_i}{\sum m_i} \quad .$$

There are alternative ways to arrive at $<\sigma_m>$, but the ones described here are among the most straightforward. This is the same as Eq. (3) (except that it is a discreet sum instead of an integral).

Various functional forms can be used to represent a specific distribution. Common ones include Gaussian, modified Gamma, and lognormal. As noted above, broader distributions will result in a larger difference in the mean particle radius for the number and mass distributions. For example, for a

lognormal distribution the mass mean radius $\langle \ln(r_m) \rangle$ is related to the number mean radius $\langle \ln(r_m) \rangle$ such that (Hoock and Sutherland, 1993)

$$\ln(r_m) = \ln(r) + 3(\ln\sigma)^2,$$

where $\ln\sigma$ is the full-width-half-maximum of the distribution. Obviously, similar expressions connecting the mass and number means exist for other distribution functions.

Appendix B

CALCULATED EXTINCTION FOR GASES: A POSSIBLE ALTERNATIVE TO POWDERS

Many molecular gases exhibit strong absorptions in the mid-infrared and these may be viable obscurant materials. Absorptions for gas phase molecules are spectrally narrow (approximately 100 cm^{-1} or 0.1 μm at 3 μm) so that the obscuration band (3-5 or 8-12 μm) averaged extinction is low. It might be possible to use a combination of gases with different vibrational frequencies and/or different isotopes to cover the band of interest. To determine whether the extinction from a gas is similar to or higher than that from a powder, the absorption intensity of a gas can be converted to a mass-extinction coefficient for a direct comparison. It is then possible to determine the gas pressure needed to achieve the extinction from a powder and whether it is practical. Absorption strengths for gases are typically listed as integrated band strengths (S_v, Rao, 1976), which can be approximated as the product of the peak intensity (I_v in $atm^{-1}cm^{-1}$) and the bandwidth ($\Delta\nu$, cm^{-1}); for a band with a Gaussian bandshape (i.e., inhomogenously broadened),

$$S_v = \left[\frac{\pi}{4\ln 2}\right]^{\frac{1}{2}} I_v \Delta\nu \quad .$$

The mass-extinction coefficient is the same quantity as the intensity expressed in different units. The conversion from intensity in $atm^{-1}cm^{-1}$ to σ_m in m^2/g is

$$\sigma_m = \frac{2.2 I_v}{M} \quad .$$

For the ν_3 band of N_2O (near 2200 cm^{-1}), for example, $S_v = 1800$ $atm^{-1}cm^{-1}$ (Rao, 1976). Since $\Delta\nu$ is approximately 100 cm^{-1}, $I_v = 18$ cm^{-1} and $\sigma_m = 0.9$ m^2/g. This is a respectable value for σ_m. The questions now arise: Is the same mass loading possible as for a powder? Is there a way to extend the extinction to all or most of the spectral band? A pressure of 200 atm of N_2O is the same as the packing density for graphite, 0.4 g/ml so that it would yield a comparable extinction to that of graphite, but only at the peak wavelength. The primary drawback with gases is achieving the spectral coverage to have high extinction throughout the targeted obscuration spectral band. Assuming a typical gas absorption bandwidth of 0.1 μm, the spectral bands at 3-5 and 8-12 μm would require at least 20 and 40 times atmospheric pressure, assuming gases could be found that span the spectral band. The prospects are dim for finding enough gases with strong absorption that cover the spectral regions. There is a better chance of this for the long wavelength band since there are more molecules that absorb strongly in that band. In this respect, the best obscurant powders have broad (electronic) absorptions so that the band-averaged σ_m is not much different than the peak σ_m.

Water mist is another possible alternative to powders. A practical advantage for a naval obscurant material is that there is an unlimited source just overboard. This obviously makes it much easier to maintain the obscuration with a continuous mist stream generated by pumping the water through a nozzle.

The extinction coefficients have been calculated as part of an NRL fire suppression study (Ladouceur, 1999). The availability may also compensate for any deficiencies in the mass-extinction coefficients compared to powders.

Appendix C

CALCULATED MASS-EXTINCTION COEFFICIENTS FOR SILICA, ALUMINA, AND SILICON CARBIDE

As stated above, Mie calculation were performed for silica, alumina, and silicon carbide. Optical constants were obtained from Palik (1984). The results are shown in Figs. C1 and C2. First of all, σ_m for alumina is low (<1 m^2/g) throughout the spectral bands (3-12 μm) of interest, so that it is not a promising extinction material. All of these materials have an absorption in the long wavelength region. The calculations indicate that they exhibit very low extinction in the spectral region on the short wavelength side of the absorption bands. For silicon carbide, the absorption is peaked near 11 μm, and the low extinction is calculated to occur near 10 μm. This agrees closely with our extinction measurements, which exhibit a strong decrease in extinction near 10 μm, as shown in Fig. 6. Since the absorption band for silica is at a somewhat shorter wavelength, near 9.5, the decrease occurs primarily outside or at the edge of the long wavelength band and there is a predicted strong extinction peaked at 9 μm. At the peak, σ_m is about 1.5 m^2/g, and it is about 0.5 m^2/g from 8.5 to 10 μm. Silica has the highest *calculated* mass extinction for the long wavelength band of the materials calculated in this study. Silica was found to have among the weakest extinction in the field test; this is primarily because of its very low packing density, as demonstrated in Table 4. The results of the field test did indicate, however, that the obscuration for silica is better in the long band than in the short band. Especially for mass-limited applications, and for those that emphasize the long wavelength band, it may be worth reconsidering silica as an obscuration material.

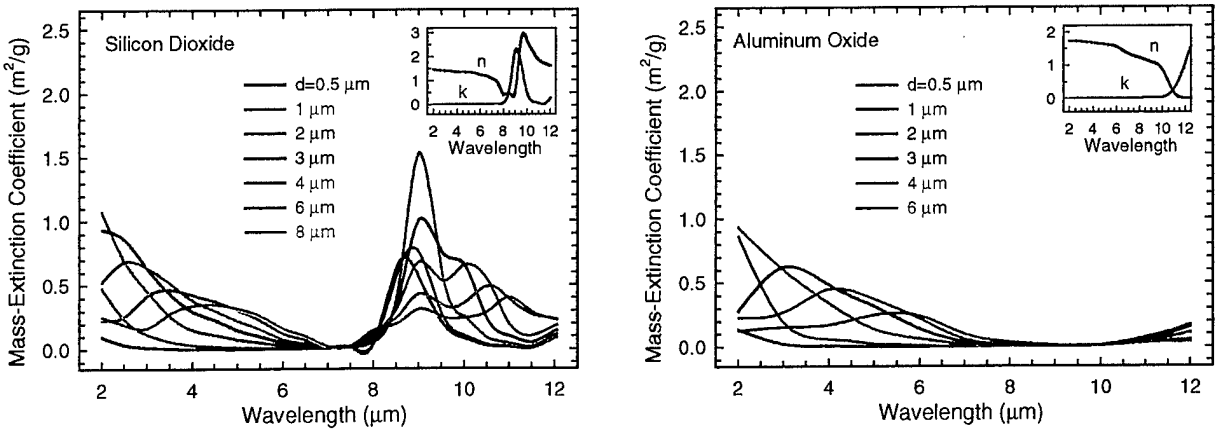

Fig. C1 – Calculated mass-extinction coefficient for silicon dioxide (left panel) and aluminum oxide (right panel) as a function of wavelength for several particle diameters

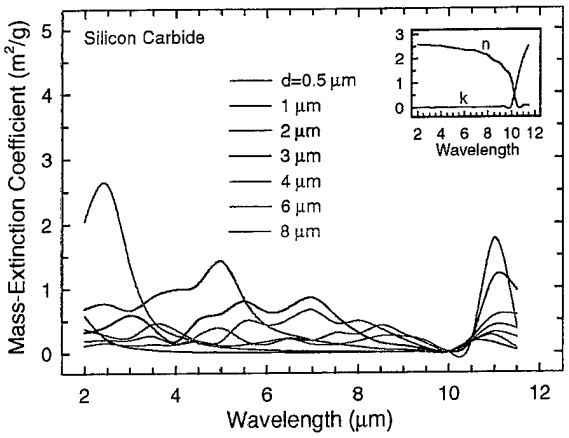

Fig. C2 — Calculated mass-extinction coefficients for silicon carbide as a function of wavelength for several particle diameters